Electromagnetic corrections to $K\to\pi\pi$. II. Dispersive matching

Vincenzo Cirigliano*
Dipartimento di Fisica dell'Universitàand I.N.F.N., Via Buonarroti, 2 56100 Pisa (Italy)

John F. Donoghue† and Eugene Golowich‡
Department of Physics and Astronomy, University of Massachusetts, Amherst, Massachusetts 01003
(Received 24 September 1999; published 13 March 2000)

We express the leading electromagnetic corrections in $K\to\pi\pi$ as integrals over the virtual photon squared momentum Q^2. The high Q^2 behavior is obtained via the operator product expansion. The low Q^2 behavior is calculated using chiral perturbation theory. We model the intermediate Q^2 region using resonance contributions in order to enforce the matching of these two regimes. Our results confirm our previous estimates that the electromagnetic corrections provide a reasonably small shift in the $\Delta I=3/2$ amplitude.

PACS number(s): 13.40.Ks, 13.25.Es

I. INTRODUCTION

In the preceding paper [1], we calculated the leading electromagnetic corrections to $K\to\pi\pi$ nonleptonic decays within chiral perturbation theory (ChPT).[1] The only hadronic degrees of freedom were the pseudoscalar mesons. Loop integrals were analyzed in terms of dimensional regularization, and counterterm amplitudes were introduced to cancel all divergences. The finite counterterms parametrize the short distance effects of heavy degrees of freedom. Our ChPT analysis yielded effects which were estimated to be at the several percent level. Unfortunately, because of the presence of many unknown finite counterterms, the results were accompanied by error bars as large as the signals.

Method of dispersive matching

In this paper we extend the previous calculation to higher energies by using a ''dispersive matching'' approach. Here, active degrees of freedom include not only the ground state pseudoscalar mesons but also the spin-zero and spin-one low-lying meson resonances. Amplitudes are expressed as integrals over the virtual photon Euclidean squared momentum Q^2. Within chiral perturbation theory, the Q^2 integral is regulated dimensionally, and unknown constants are introduced to parametrize the contributions from intermediate and high energy. In contrast, the dispersive matching approach is an attempt to construct an intermediate energy contribution that sucessfully interpolates between the low and high energy regions. This allows the full Q^2 integral to be calculated.

The $K\to\pi\pi$ amplitude with EM interactions present is given generally to order e^2 by

$$\mathcal{A}_i=e^2\int d^4q D_{\mu\nu}(q)W_i^{\mu\nu}(q,p)\quad (i=+-,00,+0), \tag{1}$$

where $D^{\mu\nu}(q)$ is the photon propagator and $W_i^{\mu\nu}(q,p)$ describes the scattering $\gamma K(p)\to\gamma\pi\pi$. Rotation to Euclidean momentum space followed by evaluation of the angular integral yields the equivalent form

$$\mathcal{A}_i=\frac{\alpha}{4\pi}\int dQ^2 W_i(Q^2)\quad (i=+-,00,+0). \tag{2}$$

To determine the $K\to\pi\pi$ amplitudes to order e^2p^2 in chiral power counting requires knowing $W_{\mu\nu}(q,p)$ [or equivalently $W(Q^2)$] at order p^2 and for all values of Q^2. We have rigorous information on $W_{\mu\nu}(q,p)$ only in the two asymptotic regimes of (i) low Q^2, where ChPT provides the appropriate couplings, and (ii) high Q^2, where the quark degrees of freedom couple to the photon according to the standard electroweak theory. Our goal will be to match these regions.

Consider the process of building $W(Q^2)$ from the low-Q^2 end. In principle we can use ChPT to generate $W_{\mu\nu}(q,p)$ to order p^2Q^{2n}. At the lowest energies, the dominant contribution is from the ground state mesons. At intermediate energies resonance degrees of freedom become active, and we can use effective Lagrangians to describe their interactions. Such resonance contributions serve to soften the polynomial behavior as Q^2 increases [2]. Eventually, the low or intermediate Q^2 description is matched to the high-Q^2 effects of Fig. 2.

Neither of the short distance contributions depicted in Fig. 2 plays a dynamical role in the radiative problem but for different reasons. The process of Fig. 2(a) leads merely to an overall shift in the strength of the weak interaction but does not give rise to mixing between the isospin amplitudes. The electroweak penguin operators of Fig. 2(b) do contribute to $K\to\pi\pi$ decay, but are found to be quite small [2] and so are

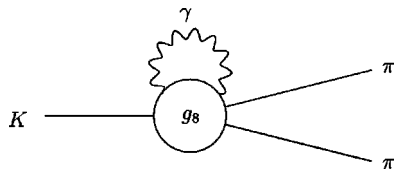

FIG. 1. Leading electromagnetic correction to $K\to\pi\pi$.

*Email address: vincenzo@het2.physics.umass.edu
†Email address: donoghue@physics.umass.edu
‡Email address: golowich@physics.mass.edu

[1]By ''leading'' is meant the component which arises from electromagnetic corrections to the (large) $\Delta I=1/2$ amplitude (cf. Fig. 1). This approach will be followed here.

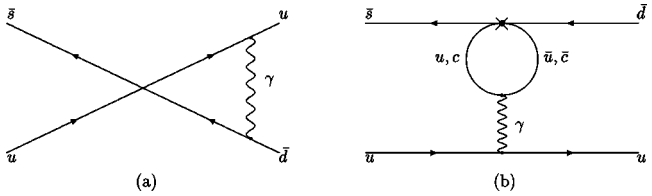

FIG. 2. High-Q^2 electroweak dynamics of quarks.

neglected in the work reported here. Physics of the low-to-intermediate Q^2 region is therefore the dominating influence in our calculation.

In Sec. II, we define the various interaction Lagrangians which are needed in the course of the calculation. We present a detailed account of the calculational program in Sec. III, from its content through to the results and some phenomenological implications. We pay particular attention to the uncertainties inherent in our calculation, and attempt to provide realistic error estimates. Final remarks appear in Sec. IV.

II. EFFECTIVE LAGRANGIANS

Our starting point will be a tree level calculation of the $\{W_i^{\mu\nu}(Q^2)\}$ including as intermediate states the ground state mesons and the low lying resonances. Their interactions are dictated by the lowest order chiral Lagrangians (of order p^2). Specifically, in the resonance sector we include the vector (V), axial vector (A), scalar (S) and pseudoscalar (P) octets and the scalar (S1) and pseudoscalar (P1) singlets.

A. Ground state mesons

The $|\Delta S|=1$ octet Lagrangian which governs the spinless ground state mesons begins at chiral order p^2,

$$\mathcal{L}_8^{(2)}=g_8\mathrm{Tr}(\lambda_6 D_\mu U D^\mu U^\dagger), \tag{3}$$

with $g_8\simeq 6.7\times 10^{-8}F_\pi^2$ and $U\equiv\exp(i\lambda\cdot\Phi)$. The corresponding $\Delta S=0$ strong and electromagnetic Lagrangian is

$$\mathcal{L}_{\mathrm{str}}^{(2)}=\frac{F_\pi^2}{4}\mathrm{Tr}(D_\mu U D^\mu U^\dagger)+\frac{F_\pi^2}{4}\mathrm{Tr}(\chi U^\dagger+U\chi^\dagger), \tag{4}$$

where $\chi\equiv 2B_0\,\mathrm{diag}(m_u,m_d,m_s)$ and $D_\mu U\equiv\partial_\mu U+ie[Q,U]A_\mu$, with A_μ being the photon field.

B. Spin-one resonances

The spin-one vector and axial vector resonances which enter our calculation are represented respectively by the field matrices $R_{\mu\nu}=V_{\mu\nu},A_{\mu\nu}$:

$$V_{\mu\nu}=\begin{bmatrix}\rho^0/\sqrt{2}+\omega_8/\sqrt{6} & \rho^+ & K^{*+}\\ \rho^- & -\rho^0/\sqrt{2}+\omega_8/\sqrt{6} & K^{*0}\\ K^{*-} & \overline{K}^{*0} & -2\omega_8/\sqrt{6}\end{bmatrix}_{\mu\nu} \tag{5}$$

and

$$A_{\mu\nu}=\begin{bmatrix}a_1^0/\sqrt{2}+f_1/\sqrt{6} & a_1^+ & K_1^+\\ a_1^- & -a_1^0/\sqrt{2}+f_1/\sqrt{6} & K_1^0\\ K_1^- & \overline{K}_1^0 & -2f_1/\sqrt{6}\end{bmatrix}_{\mu\nu}. \tag{6}$$

The normalization of $R_{\mu\nu}$ is given by

$$\langle 0|R_{\mu\nu}|R(p,\lambda)\rangle=\frac{i}{M_R}[p_\mu\epsilon_\nu(p,\lambda)-p_\nu\epsilon_\mu(p,\lambda)]. \tag{7}$$

Analogous to interactions among the spinless ground-state mesons, interactions of the resonances are likewise given in terms of effective Lagrangians [4]. For $\Delta S=0$ vertices we have

$$\mathcal{L}_{\mathrm{str}}^{(R)}=\frac{F_\mathrm{V}}{2\sqrt{2}}\mathrm{Tr}(V_{\mu\nu}f_+^{\mu\nu})+i\frac{G_\mathrm{V}}{2\sqrt{2}}\mathrm{Tr}(V_{\mu\nu}u^\mu u^\nu)+\frac{F_\mathrm{A}}{2\sqrt{2}}\mathrm{Tr}(A_{\mu\nu}f_-^{\mu\nu}), \tag{8}$$

where

$$U=uu,\quad u_\mu=iu^\dagger D_\mu U u^\dagger,$$
$$f_\pm^{\mu\nu}=u^\dagger F^{\mu\nu}u\pm uF^{\mu\nu}u^\dagger,\quad F^{\mu\nu}=eQ(\partial^\mu A^\nu-\partial^\nu A^\mu). \tag{9}$$

The couplings F_V,G_V,F_A have the numerical values [3]

$$F_V\simeq 0.154\ \mathrm{GeV},\quad G_V\simeq\frac{F_\pi^2}{F_V},\quad F_A\simeq(F_V^2-F_\pi^2)^{1/2}. \tag{10}$$

Although the effective Lagrangian used to describe $|\Delta S|=1$ interactions of the resonances is given most generally by [5]

$$\mathcal{L}_{\rm R}=\sum_{k=1}^{10} g_k^{(\rm R)}K_k^{(\rm R)}, \tag{11}$$

only four of the ten possible operators are relevant to our $K\to\pi\pi$ analysis,

$$K_1^{(\rm R)}={\rm Tr}(\Delta[R_{\mu\nu},f_+^{\mu\nu}]_+),\quad K_2^{(\rm R)}={\rm Tr}(\Delta[R_{\mu\nu},f_-^{\mu\nu}]_+),$$
$$K_5^{(\rm R)}=i{\rm Tr}(\Delta[R_{\mu\nu},[u^\mu,u^\nu]]_+),\quad K_6^{(\rm R)}=i{\rm Tr}(\Delta u_\mu R_{\mu\nu}u_\nu), \tag{12}$$

where $\Delta=u^\dagger\lambda_6 u$. Use of the $\{K_k^{(\rm R)}\}$ introduces eight couplings $\{g_k^{(\rm R)}\}$ ($R=V,A$ and $k=1,2,5,6$) into the calculation. It is convenient to convert these to dimensionless quantities

$$g_k^{(\rm V)}=\frac{g_8F_V}{F^2}\overline{g}_k^{(\rm V)},\quad g_k^{(\rm A)}=\frac{g_8F_A}{F^2}\overline{g}_k^{(\rm A)}\ \ (k=1,2,5,6). \tag{13}$$

C. Spin-zero resonances

Finally, we list effective Lagrangians for the spinless resonances, including the octet scalars S, the singlet scalar S_1 and their pseudoscalar analogues P and P_1. We begin with the strong Lagrangians,

$$\mathcal{L}_{\rm str}^{(\rm scalar)}=c_d{\rm Tr}(Su_\mu u^\mu)+c_m{\rm Tr}(S\chi_+)+\tilde{c}_dS_1{\rm Tr}(u_\mu u^\mu)$$
$$+\tilde{c}_mS_1{\rm Tr}(\chi_+),$$
$$\mathcal{L}_{\rm str}^{(\rm pseudo)}=id_m{\rm Tr}(P\chi_-)+i\tilde{d}_mP_1{\rm Tr}(\chi_-), \tag{14}$$

where $\chi_\pm\equiv u\chi^\dagger u\pm u^\dagger\chi u^\dagger$. The weak Lagrangian for the octet spinless resonances is

$$\mathcal{L}_{\rm wk}^{(\rm octet)}=\sum_{i=1}^{6} g_S^iK_i^S+\sum_{i=1}^{4} g_P^iK_i^P, \tag{15}$$

where

$$K_1^S={\rm Tr}(\Delta[S,\chi_+]_+),\qquad K_2^S={\rm Tr}(S\Delta)\cdot{\rm Tr}(\chi_+),$$
$$K_3^S={\rm Tr}(\Delta[S,\chi_-]_+),\qquad K_4^S={\rm Tr}(\Delta[S,u_\mu u^\mu]_+),$$
$$K_5^S={\rm Tr}(\Delta u^\mu)\cdot{\rm Tr}(u_\mu S),\quad K_6^S={\rm Tr}(\Delta S)\cdot{\rm Tr}(u_\mu u^\mu), \tag{16}$$

and

$$K_1^P=i{\rm Tr}(\Delta[P,\chi_-]_+),\qquad K_2^P=i{\rm Tr}(\Delta P\cdot{\rm Tr}(\chi_-),$$
$$K_3^P=i{\rm Tr}(\Delta[\chi_+,P]),\qquad K_4^P=i{\rm Tr}(\Delta[P,u_\mu u^\mu]). \tag{17}$$

The weak Lagrangian for the singlets is given by

$$\mathcal{L}_{\rm wk}^{(\rm singlet)}=\tilde{g}_P^1\tilde{K}_1^P+\sum_{i=1}^{2}\tilde{g}_S^i\tilde{K}_i^S, \tag{18}$$

with

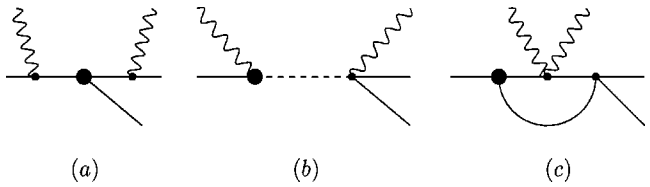

FIG. 3. Contributions to $W_i^{\mu\nu}$: (a) Born, (b) resonance, (c) loop.

$$\tilde{K}_1^S=S_1{\rm Tr}(\Delta\chi_+),\quad \tilde{K}_2^S=S_1{\rm Tr}(\Delta u_\mu u^\mu),$$
$$\tilde{K}_1^P=iP_1{\rm Tr}(\Delta\chi_-). \tag{19}$$

III. DETAILS OF THE CALCULATION

We have at hand the tools to construct reliable expressions at low and intermediate Q^2 for the $\{W_i(Q^2)\}$ functions of Eq. (2). The two major components will be the following:

(1) Tree diagrams [Figs. 3(a), 3(b)] involving exchange of the ground state pseudoscalar mesons (Born terms) and of resonances:

Within chiral perturbation theory, the vertices in the tree diagrams are described by point-like couplings at leading order. However, in QCD we know that the couplings fall off at higher Q^2. In order to incorporate this feature, we model form factor corrections to the Born terms with vector resonance contributions. The set of Born diagrams (together with insertions of meson form factors) is free of unknown parameters.

The remaining vector and axial vector resonance contributions depend on eight unknown weak couplings. Various phenomenological inputs can be used to fix them, but some remain unconstrained. In principle this part of the amplitude requires matching to the penguin short distance contribution. The requirement that matching occur successfully affords a way to further constrain the unknowns. This is further discussed in Sec. III B. The terms involving scalar and pseudoscalar resonance exchange will also contain largely unconstrained couplings. At chiral order e^2p^2, there are contributions from mass renormalizations on external legs and also from vertex-like corrections. The net effect at this order turns out to vanish.

(2) The low-energy parts of meson loop diagrams [Fig. 3(c)]:

We refer to these as the *unitarity* contributions. They constitute a genuine low-Q^2 effect distinct from that of the resonance component. In Sec. III C we shall describe such unitarity terms and provide a natural extension to all Q^2 scales, without introducing new parameters.

Before proceeding to a description of the calculation, we introduce a parametrization in terms of reduced amplitudes $\{\mathcal{C}_i\}$ and $\{\overline{W}_i\}$,

$$\delta\mathcal{A}_i^{(\rm em)}=\eta_i\frac{g_8M_K^2}{F_\pi^2F_K}\frac{\alpha}{4\pi}\mathcal{C}_i\ \text{ and }\ W_i=\eta_i\frac{g_8M_K^2}{F_\pi^2F_K}\frac{\alpha}{4\pi}\overline{W}_i \tag{20}$$

with

$$\mathcal{C}_i \equiv \int_0^\infty dQ^2 \overline{W}_i(Q^2) \tag{21}$$

and $\eta_{+-}=\eta_{00}=\sqrt{2}$ and $\eta_{+0}=1$. In addition, we partition each $\mathcal{C}$ amplitude into additive components as

$$\mathcal{C}_i = \mathcal{C}_i^{(e^2p^0)} + \mathcal{C}_i^{(\mathrm{mtchg})} + \mathcal{C}_i^{(\mathrm{unty})}. \tag{22}$$

The matching component $\mathcal{C}_i^{(\mathrm{mtchg})}$, encompassing the sum of the Born + form factor and resonance contributions, is discussed in Secs. III A and III B whereas the unitarity component $\mathcal{C}_i^{(\mathrm{unty})}$ is discussed in Sec. III C. The contribution of each component to the full amplitude is given in Table I (cf. Sec. IV).

A. Born and resonance diagrams

The class of diagrams involving exchanges of the ground state pseudoscalar mesons and of the low-lying spin-one, spin-zero resonances generates contributions at order e^2p^0 and at order e^2p^2. However, we already know the e^2p^0 contributions because chiral symmetry relates the $K\to\pi\pi$ amplitudes to the $K^+\to\pi^+$ matrix element and we have calculated this in Ref. [2]. Therefore we focus on the e^2p^2 piece in the following. We treat first in some detail the Born contributions and their corrections which arise from the insertion of meson form factors. Then we describe the parameter-dependent spin-one resonance terms and finally the spin-zero resonance terms.

1. Born and form factor contributions

The Born diagrams do not contribute to $\overline{W}_{00}(Q^2)$ (which involves only neutral particles) while giving nonzero contributions to both $\overline{W}_{+0}(Q^2)$ and $\overline{W}_{+-}(Q^2)$. For $\overline{W}_{+0}(Q^2)$ we find

$$\overline{W}_{+0}(Q^2) = \frac{3}{M_K^2} J(Q^2, M_\pi^2), \tag{23}$$

with

$$J(Q^2,m^2) = \frac{Q^2}{6m^2}\left[\left(1+4\frac{m^2}{Q^2}\right)^{3/2} - \left(1+6\frac{m^2}{Q^2}\right)\right]. \tag{24}$$

This contribution is logarithmically divergent at high Q^2 and has an infrared $1/Q$ integrable singularity at $Q^2=0$. In addition, it is suppressed by a factor of M_π^2/M_K^2. This suppression is ''accidental'' in that it is not required by any symmetry at moderate or high values of Q^2. The result is shown as the dashed line in Fig. 4.

The Born contribution to $\overline{W}_{+-}(Q^2)$ is analytically more involved. Once one extracts the infrared divergent singularity [6], it reads

$$\overline{W}_{+-}(Q^2) = C(Q^2) + S_1(Q^2, M_\pi^2) - S_2(Q^2, M_\pi^2). \tag{25}$$

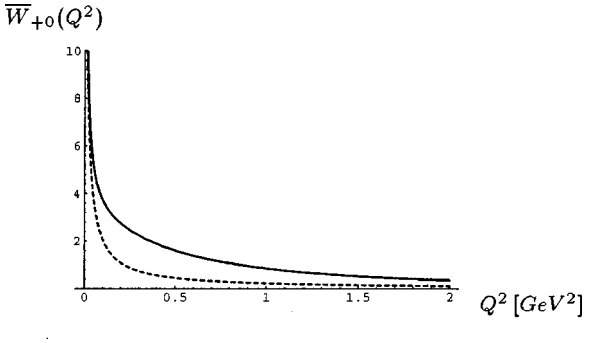

FIG. 4. Born (dashed line) and Born plus form factor (solid line) contributions.

The functions $C(Q^2)$, $S_1(Q^2,m^2)$ and $S_2(Q^2,m^2)$ are given in Appendix A, and we display $\overline{W}_{+-}(Q^2)$ as the dashed line in Fig. 5. Again, this contribution is logarithmically divergent at high Q^2. The cusp is due to the singularity related to the Coulombic rescattering.

The set of Born diagrams, required by chiral symmetry, provides a good description of the very low Q^2 region, in which the photon ''sees'' only point-like pseudoscalars. As Q^2 increases this is no longer true, and one needs to account for structure dependence in the couplings. In our model this is accomplished by introducing the low-lying resonances.

We consider first the diagrams involving pion and kaon electromagnetic form factors (saturated in this model by the vector meson resonances). This is a subclass of all diagrams required by chiral symmetry but has some nice features. It does not introduce any new parameters and improves the high-Q^2 behavior of the $\{\overline{W}_i(Q^2)\}$ while having minimal effect on the model-independent Born contributions at low Q^2. The results of this improved description are shown graphically in Figs. 4 and 5 (solid lines). The anlytical expressions are

$$\overline{W}_{+0} = \frac{M_\rho^2}{Q^2+M_\rho^2}\left[\frac{3}{M_K^2} J(Q^2,M_\pi^2) + \frac{Q^2}{Q^2+M_\rho^2}\tilde{J}(Q^2,M_K^2)\right] \tag{26}$$

and

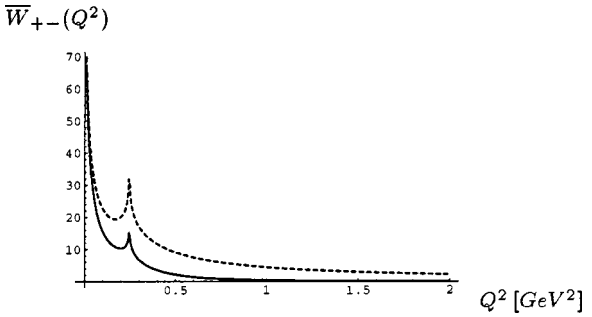

FIG. 5. Born (dashed line) and Born plus form factor (solid line) contributions.

$$\overline{W}_{+-}=\left(\frac{M_\rho^2}{Q^2+M_\rho^2}\right)^2 C(Q^2)+\frac{M_\rho^2}{Q^2+M_\rho^2}\left(\frac{M_\rho^2}{Q^2+M_\rho^2}S_1(Q^2)-S_2(Q^2)\right), \tag{27}$$

where $\tilde{J}(Q^2,m^2)$ is defined in Appendix A. Note that the new contribution to $\overline{W}_{+0}$ is not suppressed by M_π^2/M_K^2 and thus gives a substantial correction to the Born amplitude. In the case of $\overline{W}_{+-}$, however, the form factor contribution has simply the effect of softening the high-Q^2 behavior.

In principle, given the convergence properties of the ''Born + form factor'' contributions, their integrations over Q^2 can be performed up to infinity. This contribution is dominated by the low and intermediate energy regions, where the formalism is valid. This gives a first clean contribution to the $\{C_i\}$ coefficients beyond the Born approximation.

2. Resonance contributions

Our analysis contains two classes of resonances contributions, spin-one and spin-zero. We consider each one separately in the following. It turns out that the spin-zero contributions sum to zero, so that only the spin-one contributions are subject to the matching procedure of Sec. III B.

As noted earlier, chiral symmetry requires the presence of all possible vector and axial vector resonance exchange diagrams. In principle these introduce to the $\{\overline{W}_i(Q^2)\}$ a dependence on eight new parameters, describing the weak couplings of resonances. Since the analytical expressions for this large class of contributions are rather lengthy and do not illuminate the underlying physics, we refrain from reporting them here. The only feature relevant for our discussion is the general form

$$\overline{W}_i(Q^2)=\sum_\alpha \overline{g}_\alpha f_\alpha^{(i)}(Q^2). \tag{28}$$

Explicit calculation shows that the physical amplitudes actually depend only on the seven parameters

$$\overline{g}_{1,2,5,6}^{(V)},\quad \overline{g}_{5,6}^{(A)},\quad \overline{g}_2^{(A)}-\overline{g}_1^{(A)}. \tag{29}$$

Let us consider the high-Q^2 behavior of the functions $f_\alpha^{(i)}(Q^2)$ appearing in Eq. (28). Many of them go to a constant at high Q^2 or fall off as $1/Q^2$, thus leading to divergences in the integration process. Such behavior has already been observed in similar calculations of the electromagnetic mass shift of the kaon [3,7]. This simply means that the resonance dominance approximation can be trusted only up to some intermediate energy region and cannot be extended up to $Q^2\to\infty$. In Sec. III B we shall try to solve both these problems (proliferation of unknown parameters *and* high-Q^2 divergences) by requiring that the resonance amplitude contribution match the high-Q^2 behavior of the $\{\overline{W}_i(Q^2)\}$.

We consider next the spin-zero resonance contributions. In the absence of electromagnetism, the tree level exchange of the scalar and pseudoscalar resonances contributes a major part of the $K\to\pi\pi$ amplitudes at chiral order p^4 [5]. Dressing these diagrams with one virtual photon generates contributions to the amplitude $\delta\mathcal{A}_i^{\rm em}$ at orders e^2p^2 and e^2p^4. It is easy to convince oneself that diagrams with vertices coming from mass matrix Lagrangians, having already four powers of the pseudoscalar masses, will contribute at order e^2p^4 to $\delta\mathcal{A}_i^{\rm em}$. On the other hand, diagrams involving derivative vertices can give rise to effects of order e^2p^2, which we are interested in. This happens through two classes of contributions:

(1) mass renormalization on external legs and

(2) vertex correction diagrams, with virtual photons inserted according to minimal coupling.

Upon explicitly identifying and calculating these diagrams, we find an exact cancellation between the two contributions. This is identical in nature to the one found in Ref. [2] for the Born contributions at order e^2p^0. The explicit results (showing the cancellation) can be found in Appendix B.

B. Matching procedure

As stated in the above discussions, the resonance exhange contribution provides a good description for the $\{\overline{W}_i(Q^2)\}$ only up to some intermediate Q^2 region, beyond which the quark electroweak and strong interactions provide the correct framework. Experience in similar hadronic calculations has shown that the transition or matching region occurs for Q between 1.5 GeV and 2 GeV [or $2\leqslant Q^2\ ({\rm GeV}^2)\leqslant 4$]. The genuine short distance contributions were studied in the chiral limit in Ref. [2]. The outcome was that the short distance contribution to the $\{\overline{W}_i(Q^2)\}$ is rather small compared to the long distance component. Corrections to the chiral limit cannot dramatically change this qualitative picture. We can imagine assigning a 100% uncertainty to the short distance component around the central value given by the chiral limit calculation. Even in this case the long distance contribution would dominate and our ignorance of short distance physics would not significantly alter the final answer. For our purposes, the most important feature emerging from this analysis is that for $Q^2>\mu^2$ the $\{\overline{W}_i(Q^2)\}$ can be set to zero, even if we do not know the details of this transition.

On the other hand, for low and intermediate Q^2 we have reliable expressions for the $\{\overline{W}_i(Q^2)\}$, i.e., the most general parametrization implied by chiral symmetry and the low-lying part of the hadronic spectrum. The only problem with these expressions is the presence of a large number of resonance parameters unconstrained by phenomenology. In what follows we shall present a set of reasonable theoretical constraints to be imposed on them. The underlying strategy is to use on the one hand the few phenomenological inputs presently available and, on the other, to enforce the transition to the high-Q^2 region, meaning in our case that the $\{\overline{W}_i(Q^2)\}$ have to approach zero in the matching region.

1. Physical constraints on the $\overline{g}_k^{(V,A)}$

Although the $\{\overline{g}_k^{(V,A)}\}$ of Eq. (13) [see also Eq. (28)] are not predictable from a purely theoretical approach, some in-

formation can be gleaned from the phenomenology of kaon decays and assorted theoretical requirements.

The phenomenology of kaon decays, especially the radiative kaon decays, allows in principle the extraction of a large number of order p^4 constants of the weak chiral Lagrangian [5]. Assuming resonance dominance for these couplings (or, whenever possible, subtracting the short distance contribution) allows one to extract information on the resonance coupling constants. The present experimental situation does not, however, yet permit a complete implementation of this program, as only limited information is available. From $K \to 2\pi, 3\pi$ data and assuming resonance saturation of the relevant $\mathcal{O}(p^4)$ counterterms, one finds

$$4\overline{g}_5^{(V)} - \overline{g}_6^{(V)} = 0.43, \tag{30}$$

with a 20% uncertainty associated with the extraction of $\mathcal{O}(p^4)$ coupling constants [5]. The $K^+ \to \pi^+ l^+ l^-$ transition provides additional information. The decay amplitude depends on a parameter w_+, whose experimental value is $w_+ = 0.89^{+0.24}_{-0.14}$. It receives both long and short distance contributions. Using resonance saturation at $\mu_{\mathrm{ChPT}} = M_\rho$ and including explicitly the penguin contribution we find

$$\frac{1}{64\pi^2}\left(3w_+ - \log\frac{M_\rho^2}{M_\pi M_K}\right) - \frac{3F_\pi^2}{2M_\rho^2} - \frac{3}{72\pi^2}\log\frac{m_c}{M_\rho} = \frac{\sqrt{2}}{M_\rho^2}\left[\frac{F_V^2}{2}(\overline{g}_6^{(V)} - 2\overline{g}_5^{(V)}) - F_V G_V \overline{g}_1^{(V)}\right]. \tag{31}$$

At present no other phenomenological constraints are available and we thus turn to a description of the theoretical ones.

In the first place there are two conditions coming from the analysis performed in the chiral limit [2]. Let us recall the reasoning behind this. In the chiral limit, using soft-pion methods, one can relate the $K \to \pi\pi$ amplitude to the off-shell K^+-to-π^+ matrix element. Moreover the invariant amplitude $\mathcal{A}_{K^+ \to \pi^+}$ is expressible as

$$\mathcal{A}_{K^+ \to \pi^+} = \int_0^\infty dQ^2 \overline{A}_{++}(Q^2). \tag{32}$$

We get one condition by demanding that $\overline{A}_{++}(Q^2)$ vanish at infinity (no quadratic divergences). A second condition comes from demanding that $\overline{A}_{++}(Q^2)$ have no short distance component, i.e., that it vanish in the matching region defined above. Together these amount to

$$\lim_{Q^2 \to \infty} \overline{A}_{++}(Q^2) = 0 \quad \text{and} \quad \overline{A}_{++}(\mu^2) = 0. \tag{33}$$

Here we have introduced the matching scale μ and, according to our previous discussion, let it vary between 1.5 GeV and 2 GeV. The following two constraints then emerge from Eq. (33):

$$\overline{g}_1^{(V)} + \overline{g}_2^{(V)} = f_V(\mu) \equiv \frac{3}{2\sqrt{2}} \frac{F_\pi^2}{F_V^2 - F_A^2 \dfrac{M_A^2 + \mu^2}{M_V^2 + \mu^2}},$$

$$\overline{g}_1^{(A)} - 3\overline{g}_2^{(A)} = f_A(\mu) \equiv \frac{3}{2\sqrt{2}} \frac{F_\pi^2}{F_A^2 - F_V^2 \dfrac{M_V^2 + \mu^2}{M_A^2 + \mu^2}}. \tag{34}$$

Adopting the same argument, we require that $\overline{W}_{+-}(Q^2)$ and $\overline{W}_{00}(Q^2)$ vanish in the matching region:

$$\overline{W}_{+-}(\mu^2) = 0 \quad \text{and} \quad \overline{W}_{+0}(\mu^2) = 0. \tag{35}$$

We do not include the analogous condition for $\overline{W}_{00}(Q^2)$ because this function, independent of any choice of the parameters, is already very small in the matching region (it does not contain any term going to a constant for high Q^2). We believe that the conditions in Eqs. (30),(31),(33),(35) form a consistent set of physical requirements and provide us with a solid basis for any attempt to obtain a sensible answer for the so-called matching amplitudes $\{\mathcal{C}_i^{(\mathrm{mtchg})}\}$.

2. Results

The above constraints are well motivated and reasonable, but are not sufficient to completely fix all of the resonance parameters. At this stage, we could use specific models of resonance behavior to estimate the remaining parameters and then accept the range of model dependence as an estimate of our uncertainty. In doing so, however, we have found that models generally give a rather small range of results. (The exception concerns $\mathcal{C}_{+0}^{(\mathrm{mtchg})}$.) The reason is that the matching constraint is more important than the remaining parameters. Therefore, rather than using particular models we elect to follow a more model independent procedure of allowing these remaining parameters to vary completely over their reasonable physical range and to use the resulting variation to estimate the error bars for our result.

The conditions described above imply a set of linear equations for the parameters $\overline{g}_i^{(V,A)}$. In particular, we can express all the parameters in terms of just two coupling constants. That is, using what we believe are well-founded physical constraints, we select a two-dimensional hyperplane in the parameter space which we call the reduced parameter space. We chose as independent variables spanning this plane $x = \overline{g}_1^{(V)}$ and $y = \overline{g}_2^{(A)} - g_1^{(A)}$. By looking at the structure of the constraints one discovers that the other parameters depend on x, y and μ as

$$\overline{g}_2^{(V)}(x,\mu), \quad \overline{g}_{5,6}^{(V)}(x), \text{ and } \overline{g}_{5,6}^{(A)}(x,y,\mu). \tag{36}$$

We are now in a position to determine the component $\mathcal{C}_i^{(\mathrm{mtchg})}$ of the full amplitude $\mathcal{C}_i$ which is determined via matching. The construction described above allows us to express the predictions for each $\mathcal{C}_i^{(\mathrm{mtchg})}$ as a linear function of x and y:

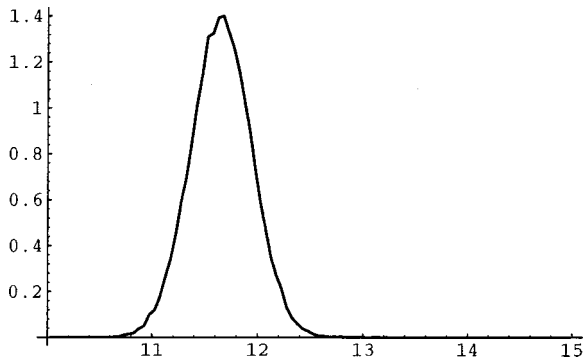

FIG. 6. Probability density function for $\mathcal{C}_{+-}^{(\mathrm{mtchg})}$.

$$\mathcal{C}_{+-}^{(\mathrm{mtchg})}(x,y)=(12.2-0.72x+0.02y)\pm|-1.0+1.35x+0.006y|,$$

$$\mathcal{C}_{+0}^{(\mathrm{mtchg})}(x,y)=(-9.2+11.47x+3.2y)\pm|-4.3+6.0x+1.0y|,$$

$$\mathcal{C}_{00}^{(\mathrm{mtchg})}(x,y)=(-0.0035-1.53x)\pm|-0.0003-0.42x|. \tag{37}$$

The uncertainties cited in Eq. (37) are associated with the matching procedure (the variation of the parameter μ). Still, this leaves freedom to pick any value for (x,y). We can further narrow our predictions by requiring that all the couplings simultaneously [as a function of (x,y)] have a ''natural'' order of magnitude, which can be shown to be $\mathcal{O}(1)$. The existence of a region in the (x,y) plane such that this happens is not guaranteed *a priori* and provides a good consistency check for our method. We call this the *physical region* in the reduced parameter space. Studying the explicit dependence of the parameters on x, y and μ we are led to define the physical region as $x{:}0.5\to1.5$ and $y{:}-1\to1$.

A first qualitative conclusion can be already drawn by looking at Eq. (37) with (x,y) restricted to the physical region and no further assumptions. The expressions show that $\mathcal{C}_{+-}^{(\mathrm{mtchg})}$ depends very weakly on the choice of (x,y) in this region, and thus we arrive at a good prediction for this parameter (see Fig. 6). $\mathcal{C}_{00}^{(\mathrm{mtchg})}$ has a moderate dependence on x and does not depend at all on y (see Fig. 7). This implies that

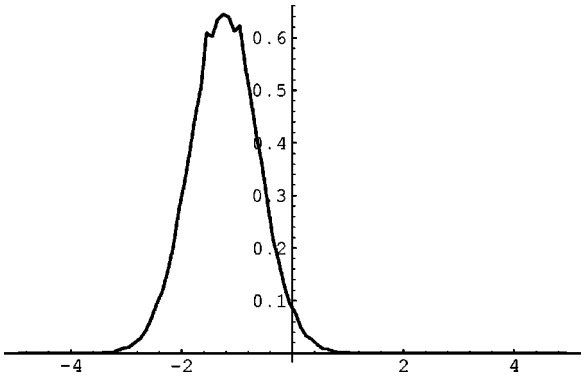

FIG. 7. Probability density function for $\mathcal{C}_{00}^{(\mathrm{mtchg})}$.

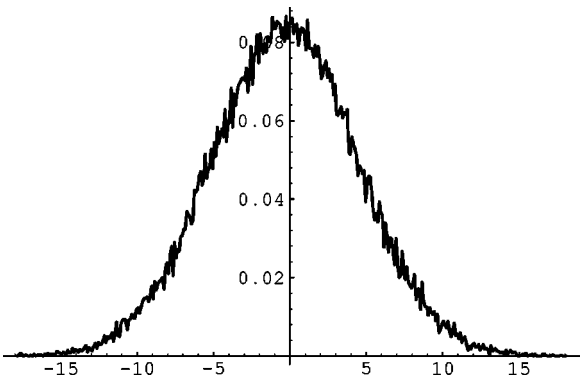

FIG. 8. Probability density function for $\mathcal{C}_{+0}^{(\mathrm{mtchg})}$.

the K^0 decay amplitudes can be predicted in our model with a reasonably small uncertainty. Problems arise in the expression for $\mathcal{C}_{+0}^{(\mathrm{mtchg})}$, which displays a fairly strong dependence on x and a moderate one on y (see Fig. 8). In this case, even confining ourselves to the physical region we obtain a spread in the answers of about 100%. The only definite prediction emerging is that this contribution is not big.

Quantitative estimates for our results and the attendant uncertainties can be obtained by constructing probability distributions for the $\{\mathcal{C}_i^{(\mathrm{mtchg})}\}$ by means of a survey of the parameter space. We scan the region defined by $\{-3\leqslant x\leqslant 3, -3\leqslant y\leqslant 3\}$ using Gaussian distributions for the input parameters. The choice of the parameters in the distributions is made in such a way to enhance contributions coming from the physical region. In view of this, we choose the central values as $x=0.8$ and $y=0$ and set variances equal to 0.4. The uncertainites cited in our results correspond to a 68% probability. Results for the $\{\mathcal{C}_i^{(\mathrm{mtchg})}\}$ are given in the second row of Table I.

C. Unitarity diagrams

Next we discuss in detail the class of diagrams schematically represented in Fig. 3(c). We are interested in the nonlocal part of these diagrams, representing the genuine propagation of mesons at low energy. The high momentum part of these diagrams produces (on general grounds [8]) local effects that can be reabsorbed into the definition of the $\mathcal{O}(p^4)$ low energy constants. In our approach, however, the local component at $\mathcal{O}(p^4)$ is implicitly contained in the resonance exchange diagrams and would show up explicitly upon expanding the resonance propagators. Keeping only the low momentum part of the meson loops ensures that the different contributions we are including in our calculation do not lead to double counting. Since the separation of local and nonlocal components in the meson loop diagrams is not free of ambiguity, we shall be careful to describe and motivate our prescription in the following.

1. Identification of the $\mathcal{O}(e^2p^2)$ contribution

Our task in the following is to identify the part in each meson loop diagram which, upon contracting the photon legs, will lead to $\mathcal{O}(e^2p^2)$ contributions. The loop contributions to $W_{\mu\nu}$ can be obtained by starting with any meson

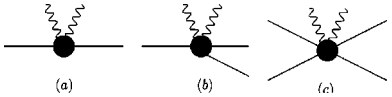

FIG. 9. Two-photon insertions: (a) $T_{\mu\nu}$, (b) $V_{\mu\nu}$, (c) $S_{\mu\nu}$.

loop diagram which contributes to $K\to\pi\pi$ and attaching two photons in all possible ways. We focus first on the subclass of diagrams obtained by attaching the following two-photon insertions:

$$T_{\mu\nu}(p,q), \quad V_{\mu\nu}(p_i,q), \quad S_{\mu\nu}(p_i,q), \tag{38}$$

as represented in Fig. 9.

For definiteness let us refer to the bare topology of Fig. 10. In this case one can insert $T_{\mu\nu}(p,q)$ on internal and external legs, $V_{\mu\nu}(p_i,q)$ in the weak vertex and $S_{\mu\nu}(p_i,q)$ in the strong vertex. The external leg insertions will generate wave function and mass renormalizations. The other insertions will give rise to diagrams like

$$D_{\rm mass}=\int d^4p\frac{V_w(p_i)V_s(p_i)}{[(k-p)^2-M_{P_1}^2][p^2-M_{P_2}^2]^2}\times\int d^4qD^{\mu\nu}(q)T_{\mu\nu}(p,q),$$

$$D_{\rm weak}=\int d^4p\frac{V_s(p_i)}{[(k-p)^2-M_{P_1}^2][p^2-M_{P_2}^2]}\times\int d^4qD^{\mu\nu}(q)V_{\mu\nu}(p_i,q),$$

$$D_{\rm strong}=\int d^4p\frac{V_w(p_i)}{[(k-p)^2-M_{P_1}^2][p^2-M_{P_2}^2]}\times\int d^4qD^{\mu\nu}(q)S_{\mu\nu}(p,q). \tag{39}$$

We wish to isolate the dominant contributions at low momentum (small p). Therefore we Taylor expand each tensor insertion around $p_i=0$ (in addition we must expand each coefficient of the Taylor series in powers of the pseudoscalar meson masses; for notational convenience we do not explicitly display this step). Considering for example the self-energy insertion, one has

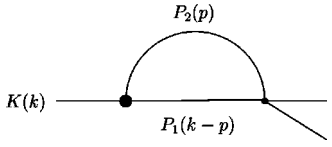

FIG. 10. Loop diagram with internal particles P_1 and P_2.

$$T_{\mu\nu}(p,q)=T_{\mu\nu}(0,q)+p_\alpha\frac{\partial T_{\mu\nu}}{\partial p_\alpha}(0,q)+\frac{1}{2!}p_\alpha p_\beta\frac{\partial^2 T_{\mu\nu}}{\partial p_\alpha\partial p_\beta}(0,q)+\cdots. \tag{40}$$

Evaluation of the integrals in Eq. (39) can be done term by term in the series. The analysis of each term is very simple. The tensor structure $\partial^n/\partial p^n T_{\mu\nu}(p,q)|_{p=0}$ factorizes out of the integration over p, and the two-photon insertion is replaced by a meson vertex of order p^n. This makes power counting transparent — after contracting the photon legs it is easy to realize that *only the first term* in the above expansion produces an effect of order e^2p^2 in the kaon ampliude. In the example considered one has

$$D_{\rm mass}=\int d^4p\ \frac{V_w(p_i)V_s(p_i)}{[(k-p)^2-M_{P_1}^2][p^2-M_{P_2}^2]^2}\times\int d^4qD^{\mu\nu}(q)T_{\mu\nu}(0,q)+\cdots. \tag{41}$$

This procedure allows us to identify and interpret the relevant contributions at order e^2p^2. The integral of $T_{\mu\nu}(0,q)$, weighted by the photon propagator in the above expression, is exactly the expression for the electromagnetic self-energy of a charged meson in the chiral limit. Thus the insertion of $T_{\mu\nu}$ in a loop diagram reproduces the effect of inserting the electromagnetic mass difference into such a loop. Equation (41) then represents the meson diagram of Fig. 10 with a mass shift insertion on the P_2 intermediate leg. Analogously, insertions of $V_{\mu\nu}$ and $S_{\mu\nu}$ yield Fig. 10 but with the weak and strong vertices replaced (respectively) by constant vertices of order e^2p^0, proportional to the chiral couplings $g_{\rm emw}$ and $g_{\rm ems}$ [1]. In other words these contributions are the counterparts to what were called *implicit* diagrams in the ChPT calculation of Ref. [1]. Their presence in the dispersive matching model is welcome because they provide imaginary parts to the amplitudes, ensuring at this order the behavior required by unitarity. These expressions when parametrized in terms of $g_{\rm emw}$ and δM_π^2, are identical to those obtained in ChPT [see Eq. (30) of Ref. [1]]. Corresponding to these contributions will, of course, also be nonvanishing real parts, whose treatment is the subject of the next subsection.

What becomes of the class of diagrams having separated photon vertices? The basic result is that they start contributing to $K\to\pi\pi$ amplitudes at order e^2p^4. A short argument for this is as follows. Upon contracting the photon legs, it is easy to recognize that these loop diagrams have the following peculiarity: their intermediate states always involve a photon (they contain one photon plus one or two pseudoscalar mesons). Let us now consider the diagrams as analytic functions of the external four momenta and analyze their imaginary parts as obtained by using the cutting equations. The above observation on the structure of the intermediate states, together with the form of the lowest order vertices and phase space, implies that the imaginary part of these diagrams is of order e^2p^4. The long distance portion of the real

part of the loop, which is all that we are interested in here, will then appear at the same chiral order.

2. Real parts of the unitary amplitudes

In the previous subsection we showed that the relevant part of the unitarity contributions at order e^2p^2 can be calculated with a simple recipe: the photon insertion factorizes out and one is left with the calculation of meson loop integrals with mass insertions on internal or external legs and weak or strong vertices replaced by constant vertices. As we have stated in the introduction to this section, we want to keep only the low energy part of these meson loops, the one that cannot be mimicked by any local counterterm or resonance-exchange diagram. We can best describe this procedure using a simple case, the two-pion loop, which also turns out to be the most relevant for the physics. The extension to all other diagrams is then straightforward.

The basic function entering the description of two-pion loops is $J_{\pi\pi}(s)$, which is given in dimensional regularization by

$$J_{\pi\pi}(M_K^2)=\frac{1}{(4\pi)^2}\left[D_\epsilon+\log\frac{\nu^2}{M_\pi^2}+1+\beta\log\left(\frac{\beta-1}{\beta+1}\right)\right], \tag{42}$$

where

$$D_\epsilon\equiv\left(\frac{2}{4-d}-\gamma+\log 4\pi+1\right), \tag{43}$$

ν is the scale parameter introduced in dimensional regularization and β is the pion velocity in the kaon rest frame. The divergent piece and the scale dependent logarithm in Eq. (42) are clearly local effects. On the other hand, the last term and the $\log M_\pi^2$ term are associated with the low energy meson propagation. Finally, an explicit cutoff calculation shows that the additive factor of one has to be included in the long-distance part. These considerations lead us to introduce a separation scale Λ_s such that the short and long distance parts are defined as

$$J_{\pi\pi}^{(\mathrm{SD})}(M_K^2)\equiv\frac{1}{(4\pi)^2}\left(D_\epsilon+\log\frac{\nu^2}{\Lambda_s^2}\right), \tag{44}$$

$$J_{\pi\pi}^{(\mathrm{LD})}(M_K^2)\equiv\frac{1}{(4\pi)^2}\left[\log\frac{\Lambda_s^2}{M_\pi^2}+1+\beta\log\left(\frac{\beta-1}{\beta+1}\right)\right]. \tag{45}$$

There is an inherent ambiguity in the separation scale Λ_s which cannot realistically be assigned a unique value. Therefore we let it range between M_K and M_ρ, associating the corresponding variation in the result as the theoretical uncertainty. These unitarity corrections come with moderate uncertainties except for the case of $\mathcal{C}_{00}$ (cf. Table I).

D. EM corrections to the isospin amplitudes

Let us consider some phenomenological consequences of our analysis. We refer the reader to Sec. II and to Sec. IV C of Ref. [1] for an introduction to formalism used in the following. In the presence of electromagnetism, the amplitudes involving charged particles ($\mathcal{A}_{+-}$ and $\mathcal{A}_{+0}$) contain infrared singularities. For each such amplitude, the infrared singularity can, on general grounds, be isolated in an exponential factor that multiplies an infrared-finite amplitude which can itself be expressed as an expansion in powers of alpha. Upon considering the emission of soft photons with energy up to some experimental scale ω, the infrared divergences disappear from the decay rate expressions, leaving ω-dependent factors $G_{+-}(\omega)$, $G_{+0}(\omega)$ which multiply the square moduli of the infrared-finite amplitudes. This process has been explicitly described in Sec. IV C in Ref. [1] for the $K^0\to\pi^+\pi^-$ mode.

Starting from the infrared-finite amplitudes in the *charge* basis, we can define the would-be isospin amplitudes from the following linear combinations:

$$\mathcal{A}_0=\frac{2}{3}\mathcal{A}_{+-}+\frac{1}{3}\mathcal{A}_{00},$$

$$\mathcal{A}_2=\frac{\sqrt{2}}{3}(\mathcal{A}_{+-}-\mathcal{A}_{00}),$$

$$\mathcal{A}_2^+=\frac{2}{3}\mathcal{A}_{+0}. \tag{46}$$

In the absence of electromagnetism and any other isospin breaking interaction, we then have $\mathcal{A}_2=\mathcal{A}_2^+$, and the amplitudes of Eq. (46) truly represent transitions to pure isospin states. Using the same logic one can perform an analysis of the unitarity condition [6], leading to the following parametrization of the $K\to\pi\pi$ infrared finite amplitudes:

$$\mathcal{A}_{+-}=(A_0+\delta A_0^{\mathrm{em}})e^{i(\delta_0+\gamma_0)}+\frac{1}{\sqrt{2}}(A_2+\delta A_2^{\mathrm{em}})e^{i(\delta_2+\gamma_2)},$$

$$\mathcal{A}_{00}=(A_0+\delta A_0^{\mathrm{em}})e^{i(\delta_0+\gamma_0)}-\sqrt{2}(A_2+\delta A_2^{\mathrm{em}})e^{i(\delta_2+\gamma_2)},$$

$$\mathcal{A}_{+0}=\frac{3}{2}(A_2+\delta A_2^{+\,\mathrm{em}})e^{i(\delta_2+\gamma_2')}. \tag{47}$$

The calculation performed in this paper gives us knowledge of the $\{\delta A_I^{\mathrm{em}}\}$. We find the shifts in the isospin amplidudes to be

$$\delta A_0^{\mathrm{em}}=\frac{\sqrt{2}g_8M_K^2}{F_KF_\pi^2}\frac{\alpha}{4\pi}\left(\frac{2}{3}\mathcal{C}_{+-}+\frac{1}{3}\mathcal{C}_{00}\right)$$
$$=(0.0253\pm0.0072)10^{-7}M_{K^0},$$

TABLE I. The $\{\mathcal{C}_i\}$ amplitudes.

	$\mathcal{C}_{+-}$	$\mathcal{C}_{00}$	$\mathcal{C}_{+0}$
e^2p^0	-3.3 ± 1.7	0	-3.3 ± 1.7
e^2p^2 (matching)	11.6 ± 0.3	-1.3 ± 0.7	-0.4 ± 4.5
e^2p^2 (unitarity)	6.5 ± 1.5	3.1 ± 1.4	-3.4 ± 1.2
Total	14.8 ± 3.5	1.8 ± 2.1	-7.1 ± 7.4
ChPT	14.1 ± 12.5	0.9 ± 6.7	-4.2 ± 4.6

$$\delta A_2^{\rm em}=\frac{\sqrt{2}g_8M_K^2}{F_KF_\pi^2}\frac{\alpha}{4\pi}\frac{\sqrt{2}}{3}(\mathcal{C}_{+-}-\mathcal{C}_{00})$$
$$=(0.0118\pm0.0063)10^{-7}M_{K^0},$$
$$\delta A_2^{+\,\rm em}=\frac{g_8M_K^2}{F_KF_\pi^2}\frac{\alpha}{4\pi}\frac{2}{3}\mathcal{C}_{+0}$$
$$=-(0.0080\pm0.0088)10^{-7}M_{K^0}. \quad (48)$$

In our numerical evaluation we have used a value for g_8 obtained from a fit to data not including radiative corrections [9]. This introduces an ambiguity in g_8 of order α which affects $\delta A_I^{\rm em}$ at order α^2 and thus is beyond the accuracy we are working at. As a by-product we obtain also the effective $\Delta I=5/2$ amplitude:

$$\mathcal{A}_{5/2}=\frac{\sqrt{2}g_8}{F_KF_\pi^2}\frac{\alpha}{4\pi}M_K^2\sqrt{\frac{2}{5}}(\mathcal{C}_{+-}-\mathcal{C}_{00}-\mathcal{C}_{+0})$$
$$=(0.0137\pm0.0097)\times10^{-7}M_{K^0}. \quad (49)$$

IV. CONCLUSIONS

The problem of determining electromagnetic corrections to nonleptonic kaon decay is a formidable one and has long resisted understanding. In this paper we have employed a ''dispersive matching'' approach which provides a framework that is, in principle, general and model independent. This dispersive setting was first advocated by Cottingham [10] and has been recently employed in Ref. [3]. At a practical level, however, a rigorous implementation of this program is plagued by a lack of sufficient input data. We have been able to overcome this obstacle by pointing out (on rather general grounds) how long range and intermediate range processes are expected to dominate the physics and then performing a calculation which incorporates the relevant ground state and resonance degrees of freedom. All possible tree-level amplitudes and a subset of loop amplitudes are taken into account. The latter component ensures that our amplitudes have the imaginary parts required by unitarity.

Contributions to the $\{\mathcal{C}_i\}$ are shown in Table I. The first row displays terms of order e^2p^0 calculated in Ref. [2]. The equal values for $\mathcal{C}_{+-}$ and $\mathcal{C}_{+0}$ are due to the absence of a $\Delta I=5/2$ component at lowest order. The second and third rows display terms at order e^2p^2, arising from the analyses done in Secs. III A, III B and in Sec. III C. The fourth row summarizes the total result obtained within the dispersive matching approach. For comparison sake, we also cite the ChPT results in the final row. We obtain EM corrections whose central values are in reasonable accord with our earlier ChPT calculation [1] but whose theoretical uncertainties are substantially smaller for the $K^0\to\pi^+\pi^-$ and $K^0\to\pi^0\pi^0$ modes. Only the $K^+\to\pi^+\pi^0$ determination produces a less precise value. It is not hard to recognize the reason for this. In our language, $\mathcal{C}_{+-}$ is dominated by the low-Q^2 Born contribution. The resonance contribution, important at intermediate Q^2, introduces only a moderate uncertainty. On the other hand, for $\mathcal{C}_{+0}$ the low-Q^2 contribution is very small, being suppressed by a factor M_π^2/M_K^2 (see Sec. III A). $\mathcal{C}_{+0}$ is thus dominated by intermediate Q^2 effects, which are plagued by a substantial uncertainty that our constraints have not completely eliminated. We could turn to model-dependent frameworks to attempt to narrow the quoted error bars. However, this apparent improvement would likely be illusory, since our understanding of models is too weak for any specific model to be trusted in a calcuation such as this. Thus we feel that our quoted error bars are a reasonable measure of present uncertainties. Note, however, that the uncertainty in $\mathcal{C}_{+0}$ is not much of a problem because of the overall smallness of the effect.

A key result of our calculations is that the electromagnetic corrections to the weak amplitudes are smaller than naive estimates might indicate. Part of the reason is the partial cancellation in the leading chiral transition that we detailed in Ref. [2]. In addition, only about a third of the overall electromagnetic effect goes into a modification of the $I=2$ final state—the rest is harmless as it contributes to the much larger $I=0$ final state amplitude. Although the work done here constitutes a crucial step in our study of EM corrections to nonleptonic kaon decay, there remain several additional issues which we shall address in a future publication [6]. Chief among these is how to correctly extract the electromagnetically corrected $K\to\pi\pi$ amplitudes from experimental data. We shall discuss the underlying theory in some detail, as well as suggesting the proper procedure to be followed in the experimental analysis. Another topic to be covered, of great current interest in studies of CP violation, involves the ratio ϵ'/ϵ. The calculation done here leads to a value for the EM correction to ϵ'/ϵ (commonly denoted as $\Omega_{\rm EM}$). We shall also provide an improved determination of the phase of ϵ'/ϵ.

ACKNOWLEDGMENTS

The research described here was supported in part by the National Science Foundation. One of us (V.C.) acknowledges support from M.U.R.S.T.

APPENDIX A: LOOP FUNCTIONS

In this appendix we give the analytic form of the functions entering in the Born term of $W_{+-}(Q^2)$. It is convenient to express them in terms of four simpler functions arising from the integration over the angular variables:

$$C(Q^2)=Q^2\Bigg[F_3(Q^2)+3F_4(Q^2)+\frac{Q^2F_4(Q^2)+F_1(Q^2,M_K^2)}{2M_K^2}\Bigg],$$

$$S_1(Q^2,m^2)=2[F_1(Q^2,m^2)-\beta^2F_2(Q^2,m^2)],$$

$$S_2(Q^2,m^2)=2\beta^2[F_1(Q^2,m^2)-F_2(Q^2,m^2)],$$

$$\tilde{J}(Q^2,m^2)=2F_1(Q^2,m^2)+F_2(Q^2,m^2). \tag{A1}$$

The F_i are

$$F_1(Q^2,m^2)=\frac{1}{2m^2}\left(-1+\sqrt{1+4\frac{m^2}{Q^2}}\right),$$

$$F_2(Q^2,m^2)=\frac{Q^2}{8m^4}\left[\left(1+\frac{2m^2}{Q^2}\right)-\sqrt{1-4\frac{m^2}{Q^2}}\right],$$

$$F_3(Q^2)=\frac{1}{\beta M_K^2Q^2}\left[\log\left(\frac{1-\beta}{1+\beta}\right)-\log\left|\frac{1-\beta\sqrt{1+\dfrac{4M_\pi^2}{Q^2}}}{1+\beta\sqrt{1+\dfrac{4M_\pi^2}{Q^2}}}\right|\right],$$

$$F_4(Q^2)=\frac{1}{2M_\pi^2Q^2}\left(1-\sqrt{\frac{Q^2}{Q^2+4M_\pi^2}}\right). \tag{A2}$$

APPENDIX B: SCALAR AND PSEUDOSCALAR RESONANCE CONTRIBUTION

Let us define the parameter $I_{\rm EM}$ as follows:

$$I_{\rm EM}=\frac{3\alpha}{4\pi}\int_0^{\Lambda^2}dQ^2. \tag{B1}$$

The scalar and pseudoscalar resonance contribution to the vertex-correction diagrams at order e^2p^2 is given by the following expressions for $\mathcal{A}_{+-}$,

$$\frac{\mathcal{A}_{+-}}{I_{\rm EM}}=\frac{4\sqrt{2}}{3F_\pi^2F_K}c_m(2g_4^S+g_6^S)\frac{M_K^2-M_\pi^2}{M_S^2}-\frac{4\sqrt{2}}{F_\pi^2F_K}\tilde{g}_4^P\tilde{d}_m\frac{M_K^2}{M_P^2}-\frac{4\sqrt{2}}{3F_\pi^2F_K}c_d\Bigg[(4M_K^2-M_\pi^2)g_1^S+3\Bigg(M_K^2+\frac{1}{2}M_\pi^2\Bigg)g_2^S\Bigg]\frac{1}{M_S^2}+\frac{\sqrt{2}}{F_\pi^2F_K}\tilde{g}_2^S\tilde{c}_m\frac{4M_K^2+2M_\pi^2}{M_{S_1}^2}+\frac{4\sqrt{2}}{F_\pi^2F_K}\tilde{g}_1^S\tilde{c}_d\frac{M_K^2-M_\pi^2}{M_{S_1}^2}, \tag{B2}$$

and for $\mathcal{A}_{+0}$,

$$\frac{\mathcal{A}_{+0}}{I_{\rm EM}}=-\frac{4}{3F_\pi^2F_K}c_mg_4^S\frac{M_K^2-M_\pi^2}{M_S^2}-\frac{4}{F_\pi^2F_K}c_d\Bigg[M_K^2g_1^S+\Bigg(M_K^2+\frac{1}{2}M_\pi^2\Bigg)g_2^S+M_\pi^2g_3^S\Bigg]\frac{1}{M_S^2}+\frac{1}{F_\pi^2F_K}\tilde{g}_2^S\tilde{c}_m\frac{4M_K^2+2M_\pi^2}{M_{S_1}^2}-\frac{4}{F_\pi^2F_K}\tilde{g}_4^P\tilde{d}_m\frac{M_\pi^2}{M_P^2}. \tag{B3}$$

The mass renormalization effect is given by the negative of this expression, with $I_{\rm EM}$ replaced by δM_π^2. However, the long distance contribution of δM_π^2 is just given by $I_{\rm EM}$ and thus these terms cancel each other. We neglect any residual intermediate energy component that may occur.

[1] V. Cirigliano, J. F. Donoghue, and E. Golowich, preceding paper, Phys. Rev. D **61**, 093001 (2000).

[2] V. Cirigliano, J. F. Donoghue, and E. Golowich, Phys. Lett. B **450**, 241 (1999).

[3] J. F. Donoghue and A. Perez, Phys. Rev. D **55**, 7075 (1997).

[4] G. Ecker, J. Gasser, A. Pich, and E. de Rafael, Nucl. Phys. **B321**, 311 (1989).

[5] G. Ecker, J. Kambor, and D. Wyler, Nucl. Phys. **B394**, 101 (1993).

[6] V. Cirigliano, J. F. Donoghue, and E. Golowich ''$K\to\pi\pi$ Final State Phases in the Presence of Electromagnetism,'' (in preparation).

[7] R. Baur and R. Urech, Nucl. Phys. **B499**, 319 (1997).

[8] J. F. Donoghue, C. Ramirez, and G. Valencia, Phys. Rev. D **39**, 1947 (1989).

[9] J. Kambor, J. Missimer, and D. Wyler, Phys. Lett. B **261**, 496 (1991).

[10] W. N. Cottingham, Ann. Phys. (N.Y.) **25**, 424 (1963).